

# Introducing yt 3.0: Analysis and Visualization of Volumetric Data

This manuscript ([permalink](#)) was automatically generated from [yt-project/yt-3.0-paper@101d453](#) on July 17, 2019.

## Authors

---

- **The yt Project**

 [XXXX-XXXX-XXXX-XXXX](#) ·  [yt-project](#) ·  [yt\\_astro](#)

NumFOCUS · Funded by Grant XXXXXXXX

- **Matthew Turk**

 [0000-0002-5294-0198](#) ·  [MatthewTurk](#) ·  [powersoffour](#)

School of Information Sciences, University of Illinois at Urbana-Champaign; Department of Astronomy, University of Illinois at Urbana-Champaign · Funded by Grant XXXXXXXX

- **Nathan J Goldbaum**

 [0000-0001-5557-267X](#) ·  [ngoldbaum](#) ·  [njgoldbaum](#)

National Center for Supercomputing Applications, University of Illinois at Urbana-Champaign · Funded by Grant XXXXXXXX

- **John A. ZuHone**

 [0000-0003-3175-2347](#) ·  [jzuhone](#) ·  [astrojaz](#)


Harvard-Smithsonian Center for Astrophysics

- **Cameron Hummels**

 [0000-0002-3817-8133](#) ·  [chummels](#)

Department of Theoretical Astrophysics, California Institute of Technology · Funded by Grant XXXXXXXX

- **Suoqing Ji**

 [0000-0001-9658-0588](#) ·  [jisuoqing](#)

Physics Department, University of California Santa Barbara · Funded by Grant XXXXXXXX

- **Meagan Lang**

 [0000-0002-2058-2816](#) ·  [langmm](#)

National Center for Supercomputing Applications, University of Illinois at Urbana-Champaign · Funded by Grant XXXXXXXX

- **Add Yourself**

 [XXXX-XXXX-XXXX-XXXX](#) ·  [yournamehere](#)

Your University

## Abstract

---

Abstract here!

## Authorship Policy

We note that the author list for this paper is, by design, extensive. We have separated the authors into those that contributed to the text (whose names are ordered **somehow TBD**) and those that are members of the `yt` community. The authors from each group have been indicated in the respective author affiliations.

This paper was developed collaboratively, using the Manubot [1] system for collaborating on and reviewing contributed text.

■ To add yourself to the author list, please follow the instructions in our [README](#).

## Introduction

---

The process of transforming data into understanding constitutes the vast majority of time, energy, and intellectual effort spent during scientific inquiry. This is true across domains, whether data is the product of a computational simulation, a telescope observation, the synthesis of sensors distributed across the Earth, or a collection of images of the human brain. Data, by themselves, do not reflect an understanding of the Universe or its underlying physical properties; rather, they are recordings, or measurements, of the state of systems as observed. Even for computational simulations, such as simulations of star formation in the galaxy, this is true: these simulations encode information about a discretization of a model, rather than the model itself.

Bridging the gap between this discretization and the physical understanding requires accessing data, manipulating and interrogating this data, and then applying to this data a sense of understanding. Somehow, bits stored on a disk must become, in our minds, a galaxy undergoing a starburst.

This process is both mediated and impeded by computational tools. When those tools align with our mental model of how data exists, they can allow us to work more efficiently, asking questions of data and building sophisticated scientific inquiry. However, when they do not, they can cause frustration, delays, and most worryingly, incorrect or misinterpreted results. When viewing this from the perspective of the landscape of inquiry, the most startling realization is that the questions a computational tool enables individuals to ask shapes the questions they think to ask.

In [2], the analysis platform `yt` was described. At the time, `yt` was focused on analyzing and visualizing the output of grid-based adaptive mesh refinement hydrodynamic simulations; while these were used to study many different physical phenomena, they all were laid out in roughly the same way, in rectilinear meshes of data. In this paper, we present the current version of `yt`, which enables identical scripts to analyze and visualize data stored as rectilinear grids as before, but additionally particle or discrete data, octree-based data, and data stored as unstructured meshes. This has been the result of a large-scale effort to rewrite the underlying machinery within `yt` for accessing data, indexing that data, and providing it in efficient ways to higher-level routines, as discussed in Section Something. While this was underway, `yt` has also been considerably reinstrumented with [metadata-aware array infrastructure](#), the [volume rendering infrastructure](#) has been rewritten to be more user-friendly and capable, and support for [non-Cartesian geometries](#) has been added.

The single biggest change to `yt` since that paper was published has not been technical in nature. In the intervening years, a directed and intense community-building effort has resulted in the contributions from over a hundred different individuals, many of them early-stage researchers, and a [thriving community of both users and developers](#). This is the crowning achievement of development, as we have attempted to build `yt` into a tool that enables inquiry from a technical level as well as fosters a supportive, friendly community of individuals engaged in self-directed inquiry.

## Community Building

---

Choosing a software package for a particular purpose involves evaluating several differentiating factors; these factors include the functionality of a package, the performance of a package, the user-friendliness, and even the ability of an individual to find help, engage with others and feel a sense of participation. **cite something here** The development, fostering and design of the community around `yt` is deemed to be both crucial to the success or failure of `yt`, and in many ways inseparable from its functionality.

## Composition

There are several rough categories of individuals engaged in development and utilization of `yt`. As a result of its API-first design, there are few if any individuals who use `yt` that do not do so through the scripting interface; this means that the vast (if not exclusive) majority of individuals who interact with the functionality in `yt` are doing so by writing their own scripts, modules, and code, and arguably engaging in a value-added development process of their own. The majority of individuals using `yt` at present are in astronomy and astrophysics, typically fields of simulation, although there is an increasing group of individuals from other domains that are participating in development and using `yt` for their own domain-specific problems.

Making the distinction somewhat more clearly, there are individuals who have built their own scripts and utilized them as well as individuals who have contributed changes or modules to the primary `yt` codebase. In addition, there is an emerging set of projects that build on `yt` as infrastructure to conduct scientific analysis. These developers are largely driven by their own pragmatic scientific needs, and they constitute the majority of developers (by number) that contribute to the code base. The majority of these individuals are early- to mid-career researchers, typically graduate students, postdocs, and assistant professors.

In recent years, there has emerged a more coherent contingency of individuals who participate in both pragmatically-focused development of modules and functionality for their own benefit as well as modules or overall improvement that is supplemental or even external to their own research agenda. These improvements include improvements to the unit handling, to the plotting code, to infrastructure for loading disparate datasets, and so on. At this time we do not know of any individuals funded to work on `yt` completely independent of a scientific or scholarly goal.

The composition of the community, particularly with a mixture of timelines for goal-setting and completion, can at times cause frustrations and difficulties. For instance, the response to “Can this feature be implemented?” often includes an invitation for the questioner to collaborate on developing that feature and submitting it to the codebase. Developing a schedule of releases is an act of consensus building, both deciding what bugs are critical to fix in the timeline of a release as well as building consensus on what features should be considered blockers for a new release. The intersection of this with academic deadlines (for instance job application season) requires balance and care.

## Types of Tasks

When evaluating the level of engagement, we consider a few different classifications of tasks that are performed by individuals in the community, and evaluate these based on how they flow into greater engagement.

- Filing issues
- Participating in mailing list discussions
- Issuing a pull request
- Writing documentation
- Participating in code review
- Drafting an enhancement proposal
- Closing bug reports

While there are other activities that individuals can participate in, these are the typical activities we see among participants in the community. The order, flowing from the first to the last, is the typical flow we see for an individual coming to participate in the community. The first step is typically to file an issue or bug report (occasionally these are requests for new features), followed by participating in development-focused discussion on mailing lists. The next level of engagement typically involves the development of a new piece of functionality, refinement of existing code, or issuing a fix for a bug or issue. These take the form of pull requests (described in greater detail [here](#)) that can be reviewed and added to the code base.

The next level of engagement centers around tasks that are not fully-aligned with pragmatic, code-driven scientific inquiry. The development of documentation is often viewed as orthogonal to the scientific process, and typically requires an iterative writing process. Participation in code review, providing comments, feedback and suggestions to other authors, is another somewhat orthogonal task; it doesn't necessarily directly benefit the developer doing the reviewing (although it might) and it does not necessarily result in academic rewards (citations, authorship, etc). But, it does arise from a pragmatic (ensuring code reliability) or altruistic (the public good of the software) motivation, and is thus a deeper level of engagement.

The final two activities, drafting enhancement proposals and closing bug reports, are the most engaged, and often the most removed from the academic motivation structure. Developing an [enhancement proposal](#) for `yt` means iterating with other developers on the motivation behind and implementation of a large piece of functionality; it requires both motivation to engage with the community and the patience to build consensus amongst stakeholders. Closing bug reports – and the development work associated with identifying, tracking and fixing bugs – requires patience and often repeated engagement with stakeholders.

## Engagement Metrics

We include here plots of the level of engagement on mailing list discussions and the citation count of the original method paper.

## Governance

## Development Procedure

---

### Answer Testing

### Code Review

### YTEP Process

## Data Objects

---

The basic principles by which `yt` operates are built on the notion of selecting data (through coarse and subsequent fine-grained indexing of data sources such as files), accessing that data in a memory-efficient fashion, and then processing that data into either a resultant set of quantitative data or a visualization.

The mechanisms by which `yt` can select data are typically spatial in nature, although several non-spatial mechanisms focused on queries can be utilized as well. These objects which conduct selection are selectors, and are designed to provide as small of an API as possible, to enable ease of development and deployment of new selectors.

Selectors require defining several functions, with the option of defining additional functions for optimization, that return true or false whether a given point is or is not included in the selected region. These functions include selection of a rectilinear grid (or any point within that grid), selection of a point with zero extent and selection of a point with a non-zero spherical radius.

The base selector object utilizes these routines during a selection operation to maximize the amount of code reused between particle, patch, and octree selection of data. These three types of data are selected through specific routines designed to minimize the number of times that the selection function must be called, as they can be quite expensive.

Selecting data from a grid is a two-step process. The first step is identifying which grids intersect a given data selector; this is done through a sequence of bounding box intersection checks. Within a given grid, the cells which are intersected are identified. This results in the selection routine being called once for each grid object in the simulation and once for each cell located within an intersecting grid. This can be conducted hierarchically, but due to implementation details around how the grid index is stored this is not yet cost effective.

Selecting data from an octree-organized dataset utilizes a recursive scheme that selects individual oct nodes, then for each cell within that oct, determining which cells must be selected or child nodes recursed into. This system is designed to allow for having leaf nodes of varying cells-per-side, for instance 1, 2, 4, 8, etc. However, the number of nodes is fixed at 8, with subdivision always occurring at the midplane.

The final mechanism by which data is selected is for discrete data points, typically particles in astrophysical simulations. At present, this is done by first identifying which data files intersect with a given selector, then selecting individual points. There is no hierarchical data selection conducted in this system, as we do not yet allow for re-ordering of data on disk or in-memory which would facilitate hierarchical selection through the use of operations such as morton indices.

**add bitmap index stuff here**

## Processing and Analysis of Data

---

### Array-like Operations

### Abstracting Simulation Types

---

### Chunking and Decomposition Strategies

Reading data, particularly data that will not be utilized in a computation, can incur substantial overhead, particularly if the data is spread over multiple files on a networked filesystem, where metadata queries can dominate the cost of IO. `yt` takes the approach of building a coarse-grained index based on the discretization method of the data (particle, grid, octree, unstructured mesh), combining this with datapoint-level indexing for selection processes.

To supplement this, methods in `yt` that process data utilize a system of data “chunking,” whereby segments of data identified during coarse-grained indexing are subdivided by one of a few different schemes and yielded to the iterating function; these schemes can include a limited number of tuning parameters or arguments. These three chunking methods are `all`, `spatial` and `io`. The `all` method simply returns a single, one-dimensional array, and the number of chunks is always exactly one; this enables both non-parallel algorithms and simple access to small datasets. `spatial` chunking yields three-dimensional arrays. For grid-based datasets, these are the grids, while for particle and octree datasets they are leaf-by-leaf collections of particles or mesh values. Optionally, the `spatial` chunking method can return “ghost zones” around regions, for computation of stencils. The final type of chunking, `io`, is designed to iterate over sets of data in a manner that is most conducive to pipelined IO. These will not always be load-balanced in size of the returned chunks, however. In some cases, `io` chunking may return one file at a time (in the case of spreading items across many different files), while in others it may be returning sub-components of a single file. This chunking type is the most common strategy for parallel-decomposition.

Necessarily, both indexing and selection methods must be implemented to expose these different chunking interfaces; `yt` utilizes specific methods for each of the primary data types that it can access. We detail these below, specifically describing how they are implemented and how they can be improved in future iterations.

## Grid Analysis

`yt` was originally written to support the Enzo code, which is a patch-based Adaptive Mesh Refinement (AMR) simulation platform. Analysis of grid-based data is the most frequent application of `yt`. While we discuss much of the techniques implemented for datasets consisting of multiple, potentially overlapping grids, `yt` also supports single-grid datasets (such as FITS cubes) and is able to decompose them for parallel analysis.

`yt` also supports other grid patch codes **insert list here**

`yt` supports several different “features” of patch-based codes. These include grids that span multiple parent objects, grids that overlap with coarser data (i.e., AMR), grids that overlap with other grids that provide the same level of resolution of data (i.e., grids at the same AMR level), refinement factors that vary based on level, and edge- and vertex-centered data. For the cases of overlapping grids (either on the same or higher refinement levels) masks are generated that indicate which data is considered authoritative.

As noted in [Data Objects](#), the process of selecting points is multi-step, starting at coarse selection that may be at the file level, and proceeding to selection of specific data points that are included in a selector. For grid-based data, the coarse selection stage proceeds in an extremely simple fashion, by iterating over flat arrays of left and right grid edges and creating a bitmap of the selected grids. Because this method – while not taking advantage of any data structures of even mild sophistication – is able to take advantage of pipelining and cache-optimization, we have found that it is sufficiently performant in most geometries up to approximately  $10^6$  grid objects. In those cases, the distinction between “wide and shallow” grid structures (where refinement occurs essentially everywhere, but not to a great degree) and “thin and deep” grid structures (where refinement occurs in essentially one

location but to very high levels), as well as the specific selection process, impact the overall performance. The second-stage selection occurs within individual grids, where points are selected based on the data point center. In the case of cell-centered data, this returns an array of size  $N$  where  $N$  is the number of points selected; in the case of 3D vertex-centered data, this would be  $(N, 8)$ .

**Andrew Myers: check this?**

Indexing grid data in `yt` is optimized for systems of grids that tend to have larger grid patches, rather than smaller; specifically, in `yt` each grid patch consists of a Python object, which adds a bit of overhead. In the limit of many more cells than grid objects, this overhead is small, but in cases where the number of grids is  $O(10^7)$  this can become prohibitive. These cases are becoming more common even for medium-scale simulations.

To address both the memory overhead and the python overhead, as well as more generally address potential scalability issues with grid selection, we have begun implementation of a more sophisticated “grid visitors” indexing and selection method. This draws on the approach used by the oct-visitors (described [below](#)). A spatial tree is constructed, wherein parent/child relationships are established between grids. Each process – selection, copying of data, generation of coordinates – is represented by an instance of a `GridVisitor` object. The tree is recursively traversed, and for all selected points the object is called. This allows grids, their relationships, and the data masks to be stored in structures and forms that are both optimized and compressed. This method is essential for scaling to a large number of grid patches; the storage requirements of a single grid patch Python object are around 1K per object (about one gigabyte per million grids), whereas the optimized storage reduces this to approximately 140 bytes (about one gigabyte per eight million grids), with further reductions possible; for selection operations, we are also able to reduce the number of temporary arrays and utilize compressed mask representation, bringing peak memory usage down further. The spatial-tree optimization substantially increases performance for “wide and shallow” dataset selection.

## Octree Analysis

## SPH Analysis

## Unstructured Mesh Analysis

## Non-Cartesian Coordinates

## Indexing Discrete-Point Datasets

---

Advances in both hardware and software facilitate astrophysical datasets of growing complexity and size. The datasets produced by numerical simulations can currently reach sizes of \$100 Tbytes split across hundreds of files [3]. For even simple analysis tasks, the cost of incrementally reading datasets this large into memory is quite high. This problem is not limited to theoretical work. During operations the Large Synoptic Survey Telescope (LSST) will produce 15 Tbytes of data each night [4]. In order to analyze such large datasets, we need innovative techniques for quickly indexing and selecting data without loading the entire dataset into memory. We present a technique for using Morton bitmap indexes to map files and accelerate data analysis.

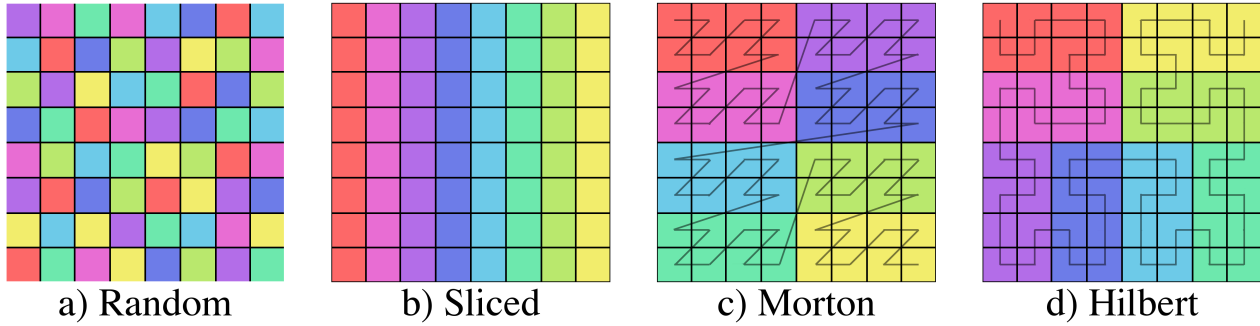
## Theory and Background

### Domain Partitioning Between Files

A common analysis task is the selection of data within a subset of the full domain; we use the term “selector” to refer to the selection operator. If the dataset is split across multiple files, either due to size constraints or to allow for parallel I/O, such selections require every file to be loaded and parsed



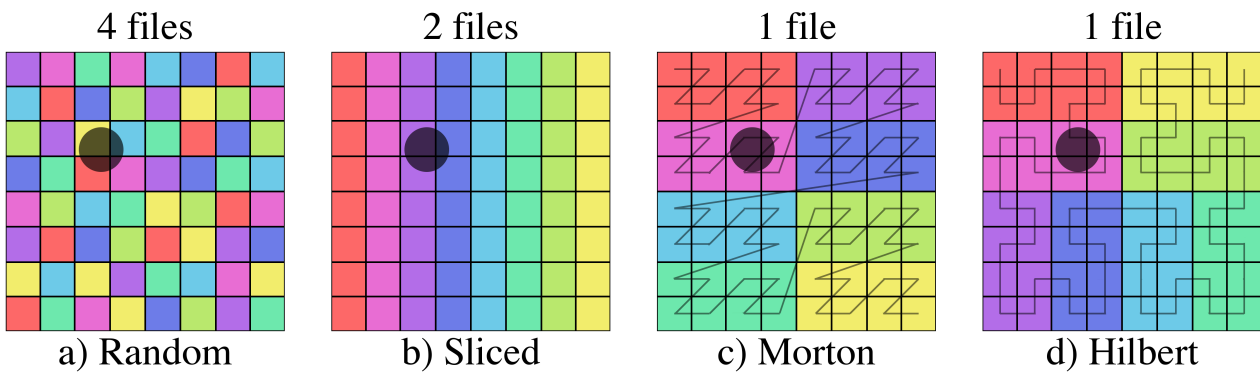
in order to assemble all of the data within the selection criteria. This process can be very costly in terms of both the memory required to store the data and the time required to read each file. However, if the contents of the files are mapped in advanced, only the files touched by the selection will need to be loaded. This is particularly effective for partitioning schemes that are localized within the domain. If each file contains data that are localized to one part of the domain, selections of contiguous sub-sections within the domain will require fewer files to be loaded. Figure 1 shows four examples of possible partitions of a two-dimensional spatial domain split equally between 8 files.



**Figure 1:** Examples of four different schemes for partitioning a 2D domain between 8 files. Each color represents a different file.

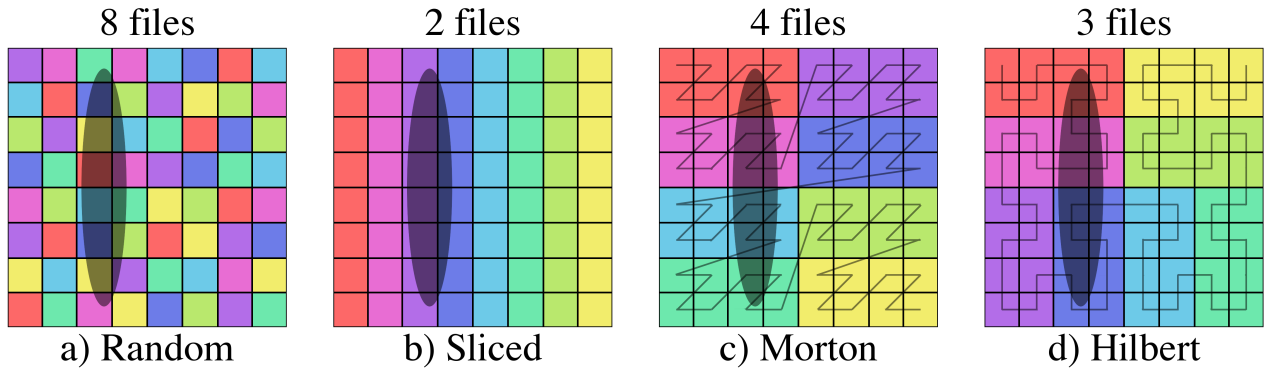
Panel (a) is an example where random parts of the domain are contained within each file. In such a case, many files will need to be loaded for contiguous selections within the domain. In panel (b), the domain was split between the files along the  $x$  dimension. Fewer files will need to be loaded for queries along the  $y$ -dimension, but contiguous selection in  $x$  will still require a greater number of files since the partition is not well localized in that dimension. Panels (c) and (d) are both examples of partitioning the domain between the files along a space filling curve [5,6]. These partitions have the greatest chance of limiting the number of files that must be loaded for a contiguous selection with slightly improved localization for the Hilbert curve. Consequently, Hilbert curves have also been used for load-balancing in parallel simulation codes like Gadget-2 [7] and RAMSES [8].

Figure 2 shows examples of three selections within the above domain partitions.



**Figure 2:** Examples of file selection for four different domain partitions and three different shaded selectors. The number of files above each images is the number of files that must be loaded in order to get all of the data within the selected region.





**Figure 3:** Examples of file selection for four different domain partitions and three different shaded selectors. The number of files above each images is the number of files that must be loaded in order to get all of the data within the selected region.

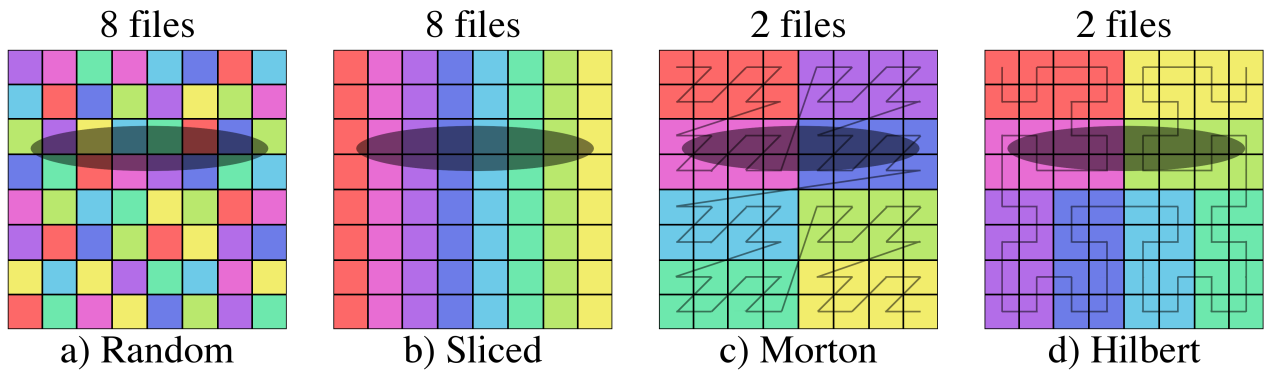


**Figure 4:** Examples of file selection for four different domain partitions and three different shaded selectors. The number of files above each images is the number of files that must be loaded in order to get all of the data within the selected region.

For the smallest selector (first row), the random domain decomposition (a) already requires half of the files to be loaded while more localized schemes require much fewer. Similarly, while the sliced domain partition (b), requires the fewest files to be loaded when the selector is oriented in the same direction as the slicing (second row), it requires *all* of the files when the selector is perpendicular to the slicing (third row). While some datasets may have information on the domain range covered by each file, the partitioning scheme used for simulation output is often decided at runtime, can be system dependent, and may be imperfect.

Files are often partitioned for parallel I/O such that each processor outputs data on the portion of the domain it is responsible for processing. To limit the cost of communication between processors, the domain will be split across processors such that neighboring processors are responsible for neighboring parts of the domain. This means that, although the overall partitioning scheme may be known for a given dataset, the exact order of the files will be dependent on the configuration of the processors at runtime.

The partitioning can also be imperfect if the domain decomposition is not perfect at the time of output. For instance, in astrophysical N-body simulations, it is possible for particles to travel from one processor's domain to another. In this case, the partition will only be perfect directly following an update to the domain decomposition.

In cases where the exact file organization is not known or imperfect, it is advantageous to map the files post-process in order to speed up selections for analysis. Although the same result can be achieved by re-sorting the data itself, creating the map can be less computationally expensive.

than re-sorting the data, can be saved for use with multiple selections, and does not required write access; this is typically not feasible, especially in the case of datasets shared by large, distributed communities.

## Morton Indices

Morton ordering maps multidimensional data onto a one-dimensional space filling curve [5]. This is done by breaking up the domain into cells where each cell's position within the  $N$ -dimensional domain can be described by  $N$  integers. The Morton index of the cell is then created by interleaving the bits of the  $N$  integers to create a single integer that fully describes the cell's position (see panel (b) Figure 5). As seen in panel (a) of Figure 5, ordering of the cells by their Morton indices forms a space filling Z-curve.

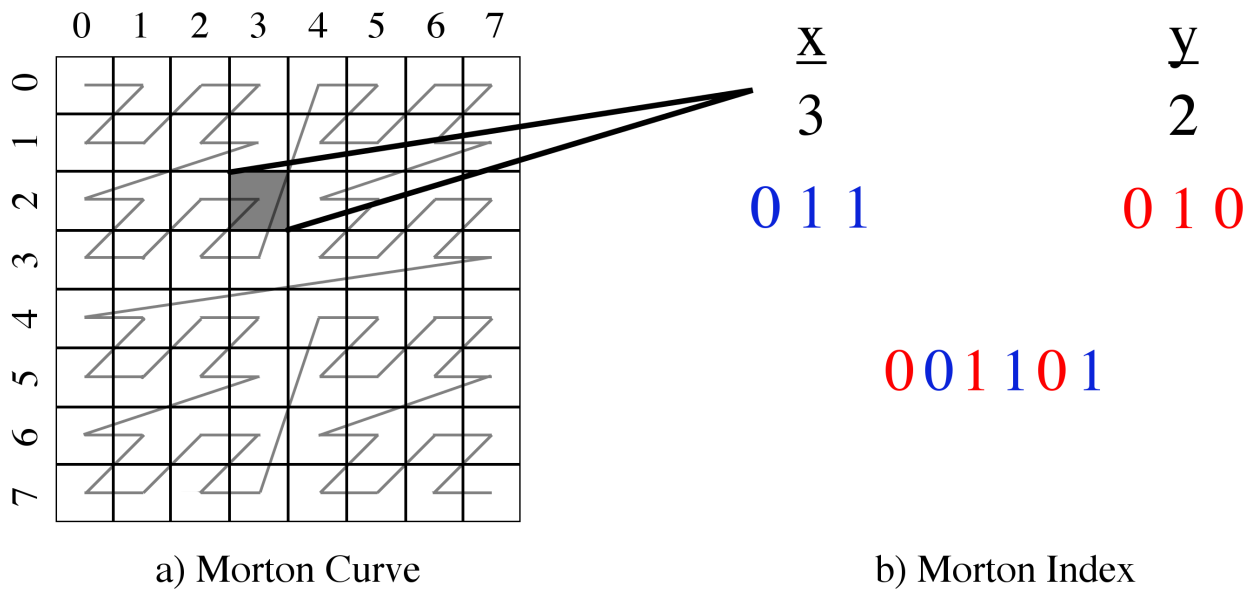


**Figure 5:** Example of 3rd order Morton curve in two dimensions. The bits of the  $x$  and  $y$  indices are interleaved to generate a single integer that fully describes the cell's location within the two-dimensional domain to within  $1/2^3$ th of the domain in each dimension.

The precision of a single Morton index is only limited by the size of the integer used to store it. For instance, 64-bit Morton indices in 3 dimensions can be localized to  $1/2^{21}$ th of the domain in each dimension ( $3 \times 21$  bits = 63 bits). If the domain is binarily divided into subcells to some order  $k$  in each dimension (i.e.  $2^{Nk}$  cells), coarser Morton indices can be obtained by simply masking lower bits. Morton ordering has been used to speed up quadtree construction [9], nearest neighbor searches [10], and range queries [11]. By recording the indices of the cells containing data from each file within a dataset, Morton indices can also be used to construct one-dimensional maps of an  $N$ -dimensional dataset that can be represented as bitmaps.

## Bitmaps & EWAH Compression

Bitmap indexes use the values of single bits within an array of bits to describe dataset properties. This form requires minimal memory and can be filtered using computationally inexpensive boolean operations. Bitmap indexes have long been popular for use with large data warehouses [12,13,14]. However, as scientific datasets have become larger and more complex, they have also begun to gain traction in a diverse array of scientific fields including geosciences [15], earth sciences, rocket science [16,17], high-energy physics [18], and combustion [19].

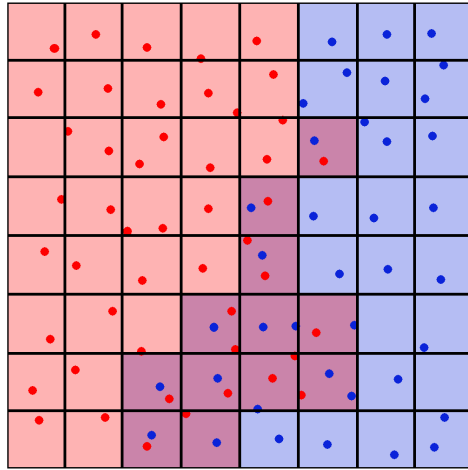
In cases where data attributes can take on a finite set of values, one bitmap is constructed for each possible attribute value. Within the bitmap each bit specifies whether or not the corresponding data point has that value. In this way, queries for data with a single attribute value require consulting only one bitmap and queries of multiple attributes/values can be done using boolean AND operations on the corresponding bitmaps. In the case of scientific data, which often contains floating point value attributes, the attributes must be binned prior to constructing the bitmaps [20,21,22]. Here, Morton indices are used to bin N-dimensional floating point data onto one-dimension. As a result, each file can be described by one bitmap.

For each file within a dataset, the Morton indices touched by the data within that file can then be stored in a bitmap index for future searches where the value of bit  $j$  indicates whether or not Morton index  $j$  is touched by the file in question. For Morton indexing of order  $k$ , this would result in a bitmap of length  $2^{Nk}$  bits per file. For large bitmaps, this can become costly in terms of memory and the time required to perform bitmap operations. However, Enhanced Word-Aligned Hybrid (EWAH) compression can be used to limit these costs, particularly when the domain is densely or sparsely populated in localized regions [23,24,25].

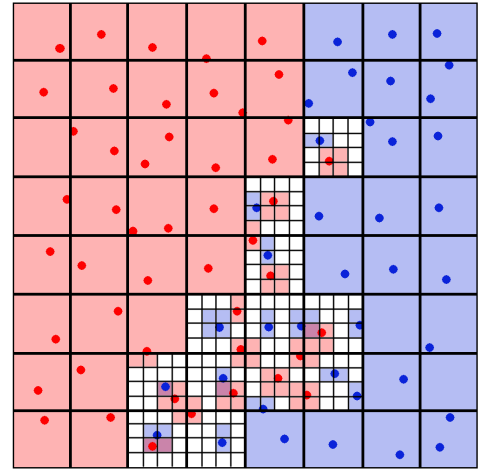
An EWAH compressed bitmap will be smaller when there are long sequences, or “runs,” of identical values. This means that an EWAH compressed bitmap will be smallest if either all or none of its bits are set. An uncompressed bitmap would require the same, maximum, amount of memory in both of these cases. The locality of Morton indices takes advantage of the EWAH compression. If there are regions of the domain that are densely/sparsely populated, there Z-order space filling curve ensures that the bits denoting those regions will be adjacent, increasing the likelihood that there will be runs of identical (set/unset) bits and limiting the size of the compressed bitmaps.

## Collisions

It is possible that two files will contain data within the same Morton cell. This would mean that any time that cell is touched by a selection, both files would need to be loaded even if the selection only touches data from one of the files. Figure 6 provides an example of collisions between two files. In panel (a) of Figure 6, purple cells are those that contain data from both files, a collision, for a 3rd order Morton index. Any selector that contained one of those cells would need to load all of the data from both files, even if it only selected part of the cell. Where the data is highly-concentrated in a central region (for instance, in a galaxy formation simulation with particles centrally-concentrated) this can mean that some regions suffer from worst-case scenario collision.



a) Coarse Collisions



b) Refined Collisions

**Figure 6:** Examples of a collision between two files. The red points and blue points are contained by two different files. The larger grid in both panels denotes the boundaries of 3rd order Morton cells. The cells containing points from either file are shaded accordingly such that cells containing points from both files are purple. The smaller grids within these cells on the right are the boundaries of 2nd order Morton cells refining the collisions.

Collisions can be limited by either increasing the order of the index or allowing for multi-resolution indexes [16,17]. Panel (b) of Figure 6 demonstrates an example of nesting a second index within cells that contain collisions. In those cells which contained collisions, a 2nd order Morton index was added. Those cells with collisions at the level of the refined index (purple cells in panel (b)) cover a much smaller portion of the domain than the cells with collisions at the level of the coarse index (purple cells in panel (a)). This means that any given selection is less likely to contain a collision and it will be less likely for a selector to require both files to be loaded unless it actually touches data from both files.

Increasing the order of the coarse index has the same effect as nesting a second refined index within cells with collisions, but can also increase the size of the resulting map and the time it takes to identify files touched by a selection. However, if the order of the coarse index is too small or the order of the refined index too large, this too can increase the cost of a selection in terms of memory and time. Section [sec:test\_order] discusses this tradeoff and how to choose index orders.

Collisions are more common for file partitioning schemes that are not localized. Figure 7 shows an example of collisions for the different partitioning schemes discussed in Section [sec:decomp].

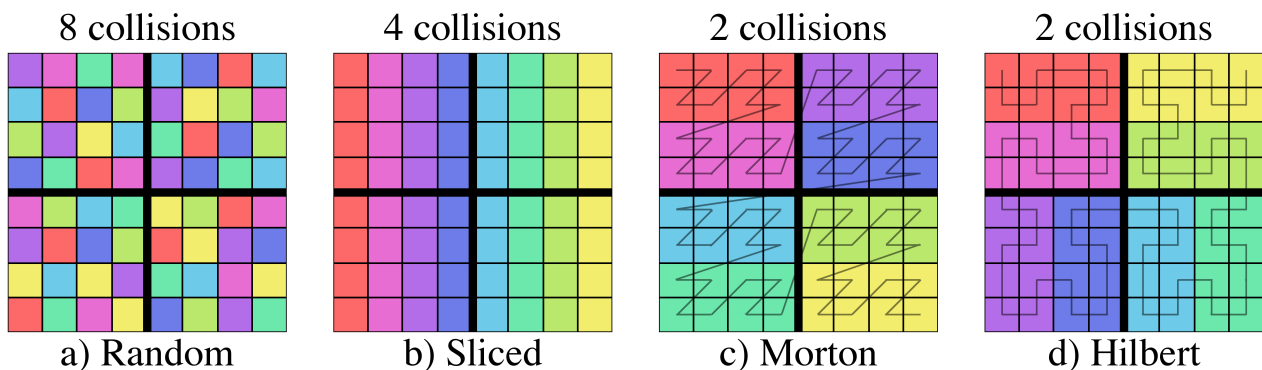


**Figure 7:** Examples of collisions for four different domain partitioning schemes. The heavy black lines denote 1st order Morton cells. The presence of more than one file (color) within a Morton cell indicates a collision.

For the random domain partition in panel (a), every cell within a 1st order Morton index will contain data from all 8 files. This means that any selection using a 1st order bitmap index will require every file to be loaded. For the more localized partitions in panels (c) and (d), only two files touch each Morton cell.

## Ghost Zones

It is often the case that, in selecting a region, additional padding around the region should be included in the selection. This is particularly useful for algorithms that need information about neighboring points in the domain [26,27,7]. For Morton indices, this is straightforward as the indices neighboring Morton cells can be found by incrementing the bits corresponding to each dimension. We have included the ability to pad selectors with some number of Morton cells referred to as ‘ghost zones’. Those files that touch ghost zones, but not the selector itself are referred to below as ‘ghost files’.

Depending on how the domain is split between files, the inclusion of ghost zones may or may not increase the number of files that need to be loaded. Figure 8 shows an example of a ghost zone around the first selector from Figure 2.

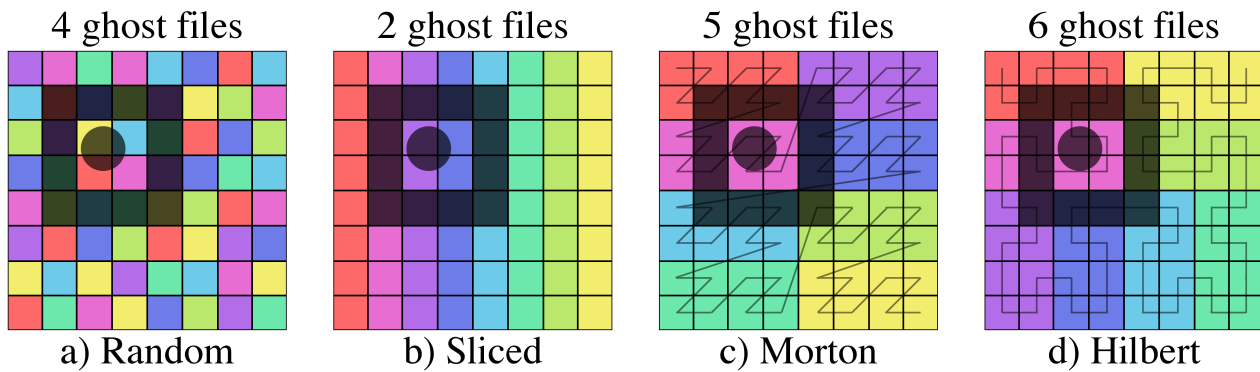


**Figure 8:** Examples of a selector ghost zone with a width of one Morton cell at an index order of 3 for four different domain partitioning schemes. The shaded circular region is the selector and the shaded box is the ghost zone. Different partitioning schemes will lead to different numbers of ghost files.

The ghost zone has a width of one Morton cell at an index order of 3 and contains the same part of the domain in each case. However, due to differences in how the domain was partitioned between the files in the four cases, the number of additional ghost files touched by the ghost zone in each case is different. This will also depend on the order of the index to which ghost zones are added. Ghost zones added at the order of the coarse index will be larger than those added at the order of the refined index and will have a higher probability of touching additional files. While including ghost zones is advantageous when neighbor info is needed, it also increases the computational cost of identifying files (see Section [sec:tests]).

## Methods

The basic procedure for constructing the bitmap index is as follows:

1. **Compute coarse indices.** For each file in the data set, read in the data and compute the indices of Morton cells at a given coarse order that are touched by data contained within that file. These coarse indices are then stored by setting the corresponding bits in an EWAH compressed bitmap.

2. **Find collisions.** The indices of coarse cells that are touched by data in more than one file (collisions) are located using bitwise operations on the file bitmaps. These indices are also stored in an EWAH compressed bitmap.
3. **Compute refined indices.** For each file in the data set, read in the data and compute the indices of Morton cells at a given refined order within coarse cells with collisions that are touched by that file. These refined indices are stored in a map from coarse Morton index to an EWAH compressed bitmap of refined Morton indices within that cell.
4. **Output bitmaps.** The EWAH compressed bitmaps for the coarse indices, refined indices, and collisions are saved to an external index file.

For large datasets and/or high levels of refinement, this can be a time consuming process; fortunately, it must only be done once. For future selections, the bitmap can be quickly loaded and used to identify files in less time than would be required to load and query each file within the dataset individually. Selection using a loaded bitmap goes as follows:

1. **Construct selector bitmap.** In the same way each file was mapped, the indices of Morton cells touched by the selector are stored in a bitmap. This is done by checking for intersection of the selector with Morton cells at the order of the coarse bitmaps. For contiguous selectors, this is done at lower order (parent) cells first and continued recursively until the order of the coarse bitmap is reached.
  - If a cell is completely within the selector, all of its child cells at the coarse order are added to the bitmap.
  - If a cell intersects the edge of the selector, child cells at increasing orders are checked until the order of the coarse bitmaps are reached. If the cell is at the coarse order and there is a collision between two files, a refined bitmap is the constructed for the selector in the same manner.
2. **Find files intersecting the selector.** Bitwise operations with the coarse file bitmaps are then used to efficiently identify files that intersect the selector within coarse cells. If the coarse cells within the intersection with a file all have collisions with other files, bitwise operations with the refined file bitmaps are then used to determine if the file is selected at the order of the refined index.

If ghost zones are desired, the neighbors of cells that intersect the edge of the selector are added to a separate bitmap. For cells without collisions, the neighbors are added at the coarse bitmap order. If there are collisions, the neighbors are added at the refined bitmap order.

## Tests

The utility of using Morton index bitmaps for mapping files to decrease query times was tested on artificial N-body simulation datasets containing  $1024^3$  points in three dimensions, distributed between 512 files. For each test a Morton index bitmap was constructed for the dataset and used to identify files touched by cube shaped three-dimensional selectors. The performance is assessed in terms of the number of files identified and the average time required to identify them across 10 runs. If fewer files are touched, fewer files will need to be loaded during analysis of a selected region and the overall fraction of time spent on I/O will be lower. If less time is required to identify the files touched by a given selector, more selections can be made using the same computational resources. This was done for varying index orders (Section [sec:test\_order]), selector sizes (Section [sec:test\_size]), and partitions of the domain between files (Section [sec:test\_decomp]).

## Index Order

## Overall Refinement

The order of the Morton indices used to map the files determines the time required to identify files and the number of collisions that will occur between files. Higher order indices will result in fewer collisions, but will take longer to query, as seen in Figure 9. Six selectors of varying sizes and positions within the domain were used to identify files based on Morton index bitmaps of varying order. The test dataset was split across the files using a Hilbert curve of order 6 with 10% scatter between Hilbert cells to simulate an imperfect domain decomposition as can occur if particle positions are updated and output prior to updating the domain decomposition.

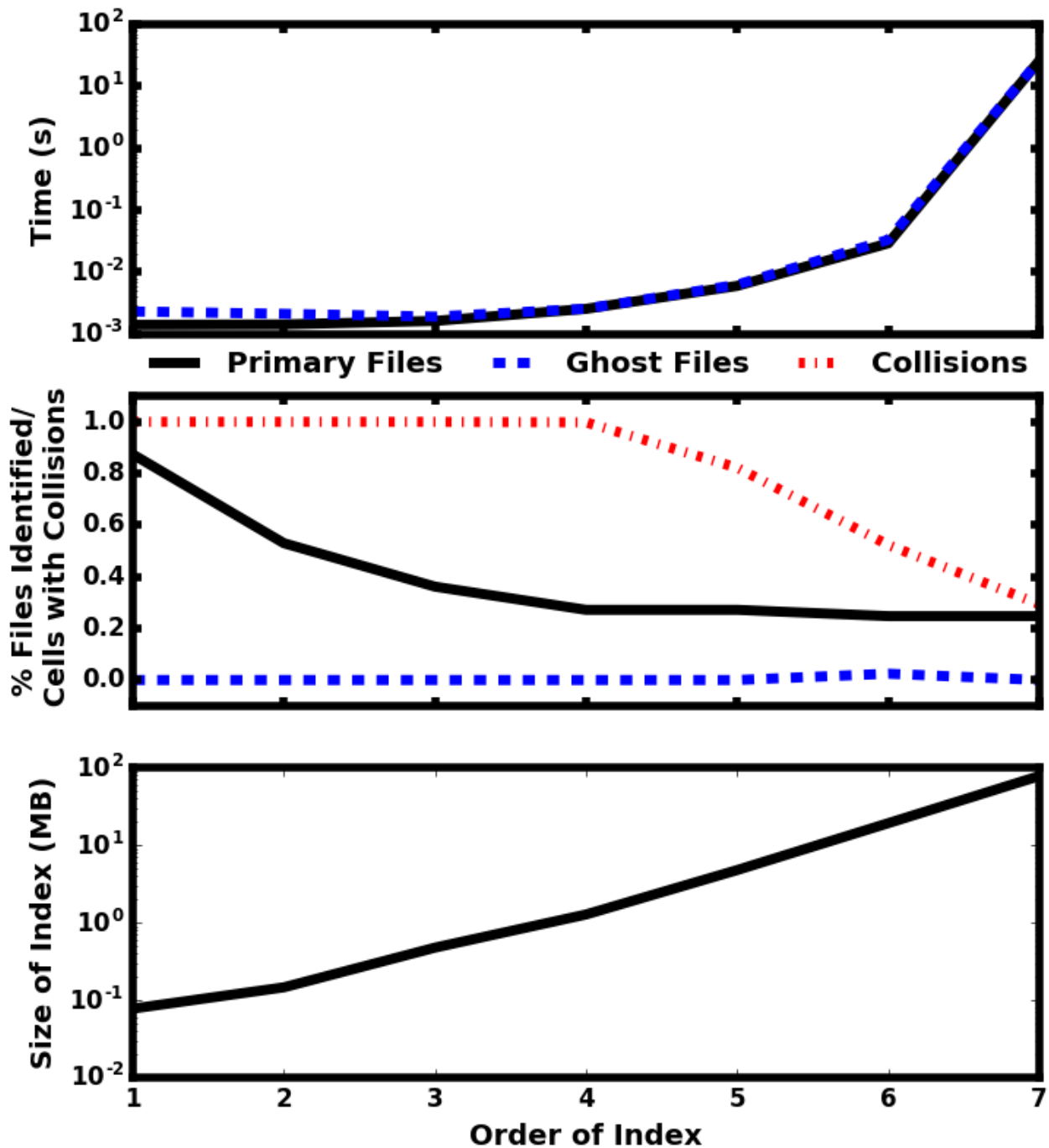


**Figure 9:** Dependence of query time (top), fraction of files selected/cells with collisions (middle), and index size (bottom) on the total refinement of the bitmap index. The solid black lines correspond to the query times and files



identified by just the selectors. The dashed blue lines correspond to the query times and additional files selected when a ghost zone with the width of one Morton cell is added around the selectors. The dash-dotted line in the middle panel shows the fraction of cells with collisions between files.

Below a bitmap index order of 4, there are collisions between multiple files within every cell, resulting in a larger number of files being identified. However, as the order increases, the number of collisions drops and the file count plateaus at  $\sim 25\%$ . This translates to a  $\sim 75\%$  reduction in the memory and time required for processing files, a significant increase in performance. For a 7th order bitmap index, selection requires  $> 100\times$  the time that the same selection took using a 6th order index, but there is no change in the number of files indicated. A 6th order index is sufficient to identify the minimal set of files touched by the selectors in this case because the dataset was partitioned between the files along a 6th order Hilbert space filling curve. While it is generally true that the time required to identify files using a bitmap index will increase exponentially with the size of the index, the order of the index that results in the minimal number of files for any dataset will depend upon how the domain is partitioned between files (see Section [sec:test\_decomp]). The memory required to store the index for the test dataset scales according to  $\propto 2^{2k}$ , for a  $k^{\text{th}}$  order index. If uncompressed bitmaps had been used instead of EWAH compressed bitmap, the memory would have scaled with the total number of cells contained within the 3-dimensional test domain ( $2^{3k}$ ).

## Collision Refinement

Increasing the refinement of the primary index does so for the entire domain and, as seen in Section [sec:test\_order1], can become costly in terms of the memory required to store the bitmap and the time required to perform operations. However, it is also possible to increase refinement by nesting a second Morton bitmap index within those cells of the primary index that contain collisions. As the nested indexes will contain a smaller portion of the domain and data, they will be less complex and can be compressed more efficiently than the primary index covering the entire domain. This enhanced compression mean that, although a greater overall number of EWAH compressed bitmaps will need to be utilized (one for the coarse index and one for each collision within the coarse index), less space will be needed to store the bitmap and bitwise operations will be faster. Figure 10 shows the results for adding a secondary index of varying order with the overall refinement order of the index (primary index order + secondary index order) held constant at 6. The test dataset and selectors applied were the same as in Section [sec:test\_order1].

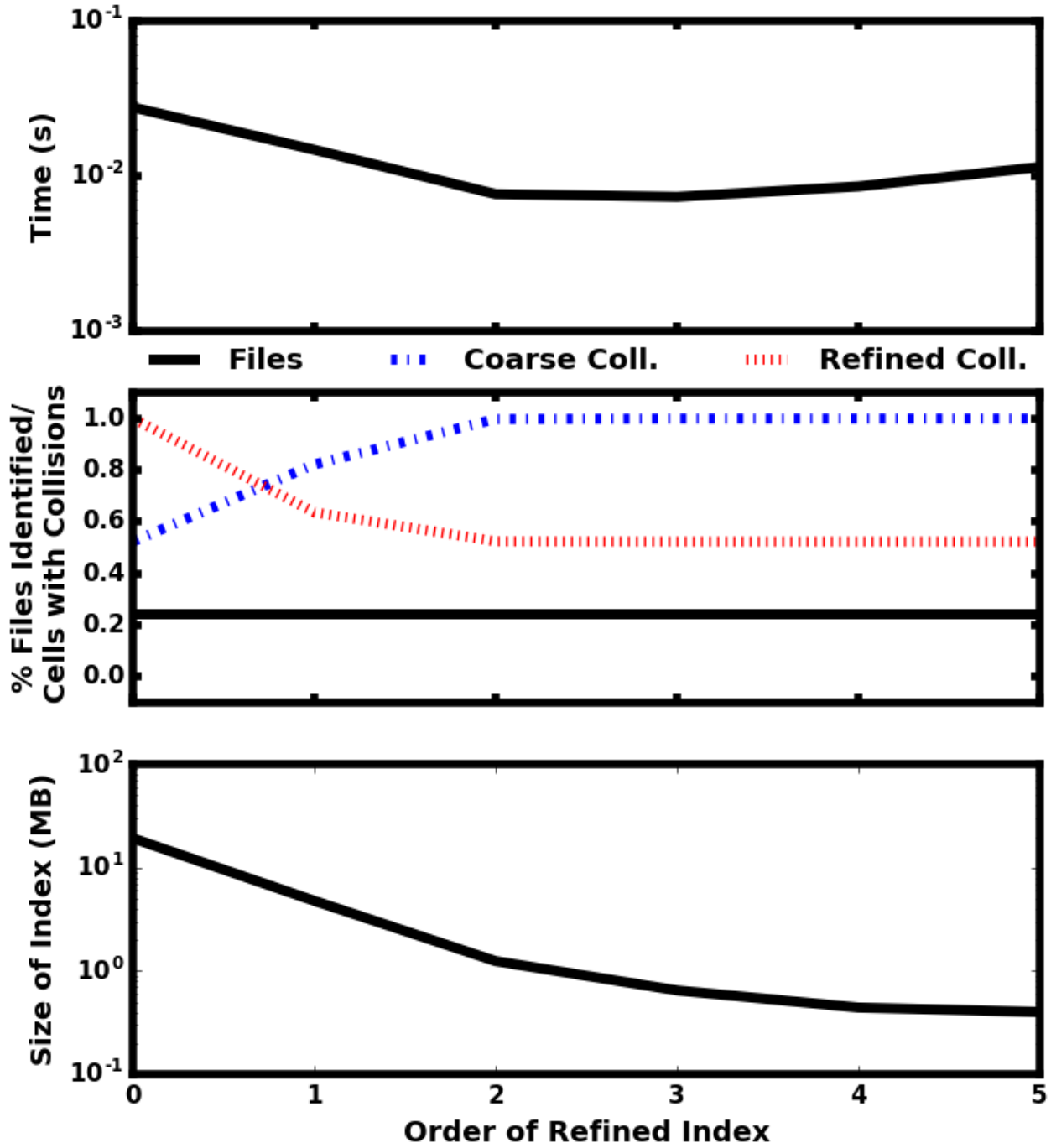


**Figure 10:** Dependence of query time (top), fraction of files selected/cells with collisions (middle), and memory required to store the index (bottom) on the order of the secondary index used to refine collisions. In the middle panel, the solid black line corresponds with the fraction of files identified, the dash-dotted blue line is the fraction of cells at the first index level that have collisions, and the dotted red line is the fraction of cells at the second index level that have collisions.

When the order of the second refined index is low, the first index is larger resulting in fewer cells with collisions at the first index and more at the second. The reverse is true when the order of second index is higher. As the overall order is held constant, the same number of files are identified regardless of the orders of the first and second indexes. The time required to identify the files is minimized when cells within the first index become saturated with collisions. For secondary indexes of order 2 or lower, the large increase in performance offered for increases in the index order results

from the reduction in the total complexity of the index which translates to shorter times for bitwise operations and less memory required for storage. Above 2nd order, the overhead from storing and accessing more complex EWAH compressed bitmaps for each collision begins to flatten the memory scaling and increase the time required for queries. However, selections using higher order secondary indices still require less time than in the case where only a single index is used.

The optimal value for the orders of the first and second indexes will depend upon the dataset in question. The density of data points within the test dataset used here is relatively uniform throughout the domain and does not need a high level of refinement at collisions. However, if a data set were less uniform with concentrations of points, the optimal order of the second index for performance may be higher.

## Selector Size

The time required to identify files touched by a selection will also depend upon the size of the region being selected. Larger selectors will intersect more indices and more files, resulting in more bitmap operations. Figure 11 shows the result from varying the selector size. The same test data set from Section [sec:test\_order] was used. A bitmap index with a 4th order primary Morton index and 2nd order secondary Morton index was used in all cases. Each cube selector was placed at the center of the domain and scaled along each dimension to some fraction of the total domain.

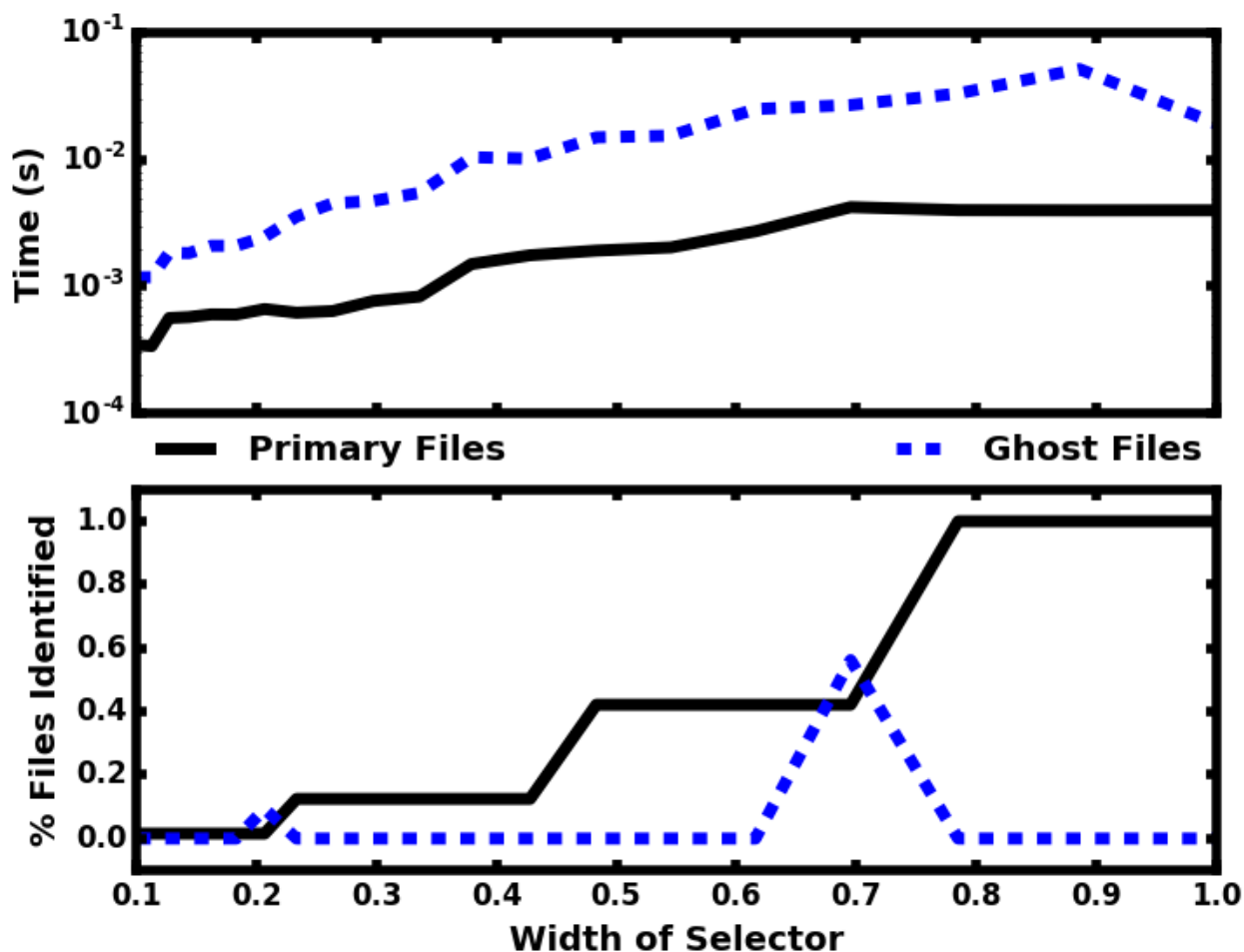


**Figure 11:** Dependence of query time (top) and number of files selected (bottom) on selector width in terms of the total domain width. The solid black lines correspond to the query times and files identified by the selectors alone. The dashed blue lines correspond to the query times and additional files identified when a ghost zone with a width of one cell is added to the selector.

As the selector increases in size, it touches a greater number of files, resulting in longer query times. The number of files touched increases in steps due to the way the test dataset was partitioned between files. Using the Hilbert curve, the domain covered by any one file is localized and will have a rectangular shape. This results in an ordered structure that is similar along all dimensions. An increase in the number of files touched indicates that the selector has grown past a file boundary in all directions. It is just prior to these jumps that ghost files are present. If the selector edge is near a file boundary, ghost zones have the potential to overlap the domains contained by neighboring files that are not already touched by the selector. For such a highly ordered dataset, the ghost zones will only identify additional files for selectors that are nearing the edges of file boundaries. However, queries including ghost zones require slightly more time even when this is not the case.

## Domain Partitioning

As discussed in Section [sec:decomp], a bitmap index is more effective in cases where the domain is partitioned between files in a localized way. If files contain non-contiguous parts of the domain, contiguous selections will require more files to be loaded. Figure [12](#) shows results for four different partitioning schemes. All four data sets cover the same three-dimensional domain with  $1024^3$  points split across 512 files. The Hilbert dataset is the same one used in previous tests (see Section [sec:test\_order] for a description). The Morton dataset is constructed in a similar way to the Hilbert dataset with file partitions occurring along a 6th order Morton curve and including a 10% scatter of points between Morton cells. The sliced dataset is partitioned in slices along one dimension with 10% scatter of points between adjacent slices. Files in the random dataset contain a random sample of points, uniformly distributed across the domain.

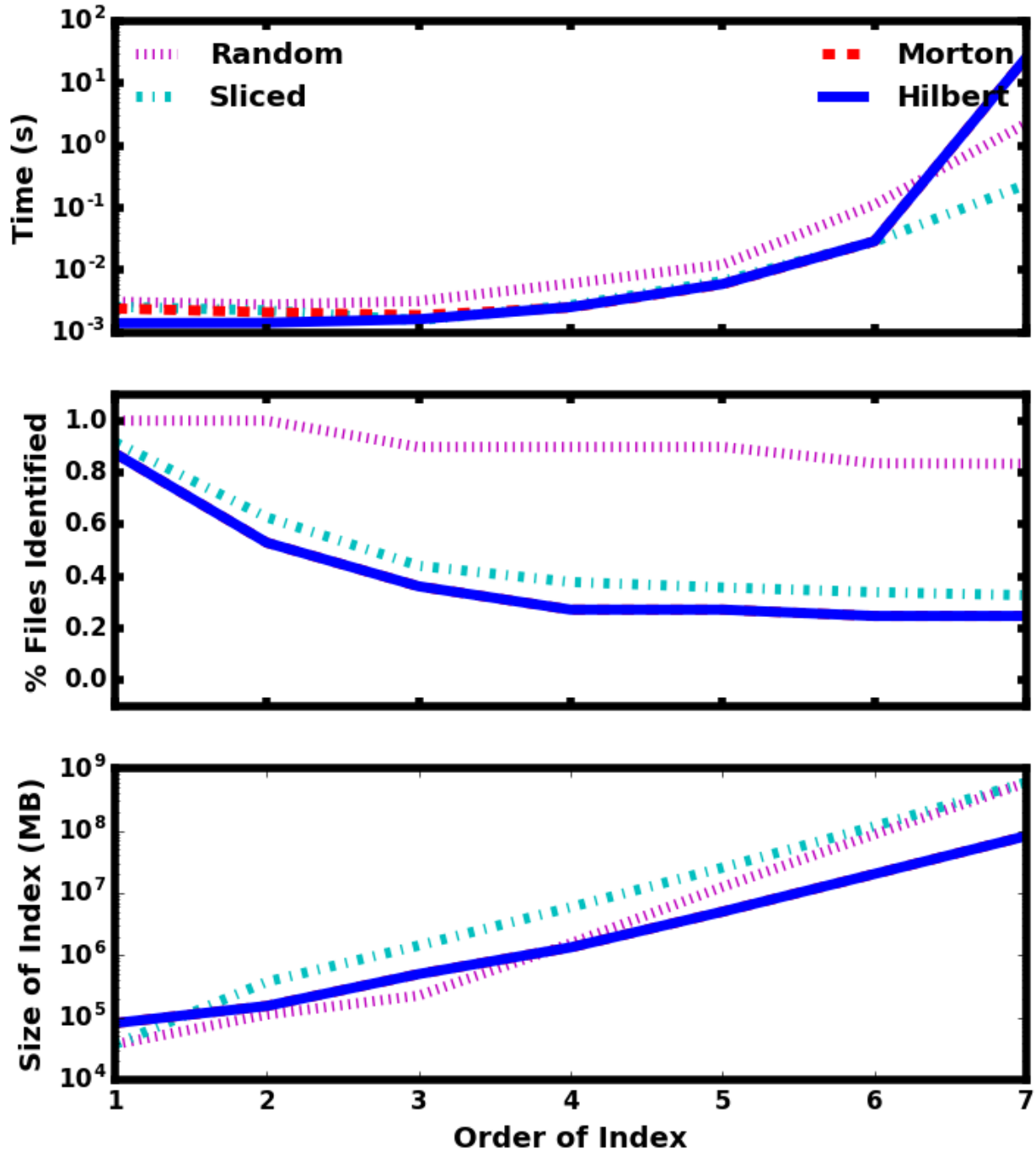


**Figure 12:** Dependence of query time (top), the number of files selected (middle), and the size of the index (bottom) on index order for different domain partitioning between files. The dotted magenta lines are for a randomly partitioned dataset, the cyan dashed-dotted lines are a dataset partitioned by equal slices along one dimension, the dashed red lines are a dataset partitioned along an 6th order Morton curve, and the solid blue lines are a dataset partitioned along a 6th order Hilbert curve.

Many more files are identified for the random dataset than those datasets with localized partitioning of the domain. Above an order of 3, very few files could be excluded for the random dataset. This was not true for the localized partitioning schemes. At the highest order, only  $\sim 20 - 30\%$  of the files within these datasets would need to be loaded in order to get all of the data within the selected regions, while  $\sim 80\%$  of the files in the random dataset would be required. The smallest fraction of files were identified for the Hilbert and Morton datasets, with a slightly greater fraction being

identified for the sliced dataset. For a 6th order index and below, queries on the Morton and Hilbert partitioned datasets are the fastest. An index order of 7 provides refinement beyond the 6th order curves used to partition the dataset between the files and the required for queries on these datasets increases dramatically. The sliced dataset performed particularly well in this case because the selectors used were cubes and did not preferentially select along any one dimension.

Overall, this technique offers a considerable improvement in performance over other methods that require reading, evaluating and discarding all of the particles.

## Summary & Discussion

Mapping files using Morton bitmap indexes speeds up analysis of large datasets split across multiple files by reducing the number of files that need to be loaded in order to perform operations on a subset of the full domain. The time required for making selections using the bitmap index is minimal for even large datasets and can be optimized by partitioning the domain between files in a localized way and using an index or indexes of appropriate order for the dataset.

Without an index, queries require loading the data contained in every file into memory and then searching the data for those points that are selected by the query. With a bitmap index, queries require loading the index, using it to identify the files touched by the query, reading in the data contained within the identified files, and searching the data for points selected by the query. In this way, the bitmap index can decrease the computational cost of reading in the data and selecting data points if it identifies a subset of the total number of files. While using an existing bitmap index decreases the time required for queries in this case, constructing a bitmap index can be more computationally expensive than directly querying the data without a bitmap index. Therefore, in the case where only a small number of selections need to be made, it will be more efficient to perform direct queries of the data than to construct and utilize the bitmap index.

Bitmap indexing is particularly useful in astronomy and astrophysics. Output from N-body simulations is often split between multiple files to take advantage of parallel I/O and the domain decomposition generally leads to localized partitioning between files [27,28,7].

Currently, this technique is most useful for datasets split across multiple files. However, it can also be applied to single files by dividing the file's contents into chunks. As in the multi-file case, the single file would need to be organized such that chunks were localized within the domain to take full advantage of the bitmaps. In addition, while the current implementation of this method is designed for three-dimensional spatial datasets like those produced by astrophysical simulations, the same methods can be applied to non-spatial datasets with arbitrary dimensionality.

## Code

These procedures have been implemented as part of the yt python package [29] in order to facilitate the analysis of large astrophysical N-body simulations; currently undergoing review for inclusion in a future version of yt (3.4 or later), our implementation is available at <https://bitbucket.org/langmm/yt-bitmap>. The open source EWAHBoolArray C++ package is used for implementing EWAH bitmaps [24,25] and exposed to Python using Cython [30].

## Acknowledgment

The authors would like to thank Daniel Lemire for his open source EWAH implementation. yt is developed by a large number of independent researchers from numerous institutions around the world. Their commitment to open science has helped make this work possible.

# Visualization and Volume Rendering

---

## Pixelizing Variable-Mesh Objects

## Higher-Order Unstructured Mesh Elements

## Software Volume Rendering

## Hardware-accelerated Volume Rendering

## Units and Quantities

---

At a basic level, `yt` is an engine for converting data dumped to disk by a simulation code into a physically meaningful result. Attaching units to simulation data makes it possible to perform dimensional analysis on the simulation data, adding additional opportunities for catching errors in a data processing pipeline. In addition, it becomes straightforward to convert data from one unit system to another.

In `yt` 3.0 we handle units in an automatic fashion, leveraging the symbolic math library `sympy`. Instead of returning a NumPy `ndarray` when users query `yt` data objects for fields, return a `YArray`, a subclass of `ndarray`. `YArray` preserves `ndarray`'s array operations, including deep and shallow copies, broadcasting, and views. Augmenting `ndarray`, `YArray` attaches unit metadata to the array data, enabling runtime checking of unit consistency in arithmetic operations between `YArray` instances, and making it trivial to compose new units using algebraic operations.

As a trivial example, when one queries a data object (here given the generic name `dd`) for the density field, we get back a `YArray`, including both the simulation data for the density field, and the units of the density field, in this case  $\text{g}/\text{cm}^3$ :

```
>>> dd['density']
YArray([4.92e-31, 4.94e-31, 4.93e-31, ...,
        1.12e-25, 1.59e-25, 1.09e-24]) g/cm**3
```

One of the nicest aspects of this new unit system is that the symbolic algebra for unitful operations is performed automatically by `sympy`:

```
>>> print dd['cell_mass']/dd['cell_volume']
[4.92e-31 4.94e-31 4.93e-31 ...
 1.12e-25 1.59e-25 1.09e-24] g/cm**3
```

`YArray` is primarily useful for attaching units to NumPy `ndarray` instances. For scalar data, we have created the new `YTQuantity` class. `YTQuantity` is a subclass of `YArray` with the requirement that the `'array data'` associated with the instance be limited to one element. `YTQuantity` is primarily useful for physical constants and ensures that the units are propagated correctly when composing quantities from arrays, physical constants, and unitless scalars:



```
>>> from yt.utilities.physical_constants import
      boltzmann_constant
>>> print dd['temperature']*boltzmann_constant
[ 1.28e-12 1.29e-12 1.29e-12 ...
 1.63e-12 1.59e-12 1.40e-12] erg
```

If a user needs the field in a different unit system, they can quickly convert using `convert_to_units` or `in_units`.

When a `Dataset` object is instantiated, it will itself instantiate and set up a `UnitRegistry` class that contains a full set of units that are defined for the simulation. This registry includes both concrete physical units like `cm` or `K` but also units symbols that correspond to the unit system used internally in the simulation.

The new unit systems let us to encode the simulation coordinate system and scaling to physical coordinates directly into the unit system. We do this via code units.

Every `Dataset` has a `length_unit`, `time_unit`, and `mass_unit`, attribute that the user can quickly and easily query to discover the base units of the simulation. For example:

```
>>> import yt
>>> ds = yt.load("Enzo_64/DD0043/data0043")
>>> print ds.length_unit
128 Mpccm/h
>>> print ds.quan(1.0, "code_length").in_units("Mpccm/h")
128 Mpccm/h
>>> print ds.length_unit.in_cgs()
5.55517285026e+26 cm
```

Optionally `velocity_unit`, `pressure_unit`, `temperature_unit`, and `density_unit` may be defined as well if the units for these fields cannot be inferred from the mass, length, and time units.

Additionally, we allow conversions to the simulation unit system. Data in code units are available by converting to `code_length`, `code_mass`, `code_time`, `code_velocity`, `code_density`, `code_magnetic`, `code_pressure`, `code_metallicity`, or any combination of those units. Code units preserve dimensionality: an array or quantity that has units of `cm` will be convertible to `code_length`, but not to `code_mass`.

On-disk data are also be available to the user, presented in unconverted code units. To obtain on-disk data, a user need only query a data object using an on-disk field name:

```

>>> import yt
>>> ds = yt.load('`Enzo_64`'/DD0043/data0043")
>>> dd = ds.all_data()
>>> print dd[('enzo', 'Density')]
[ 6.74e-02 6.12e-02 8.92e-02 ...
 9.09e+01 5.66e+01 4.27e+01] code_mass/code_length**3
>>> print dd[('gas', 'density')]
[ 1.92e-31 1.74e-31 2.54e-31 ...
 2.59e-28 1.61e-28 1.22e-28] g/cm**3

```

Here, the first data object query is returned in code units, while the second is returned in CGS units. This is because `("enzo", "Density")` is an on-disk field, while `("gas", "density")` is an internal `yt` field.

## Implementation

Our unit system has 6 base dimensions, `mass`, `length`, `time`, `temperature`, and `angle`. The unitless `dimensionless` dimension, which we use to represent scalars is also technically a base dimension, although a trivial one. For convenience, we also create dimensionless unit symbols to represent quantities like metallicity that are formally dimensionless, but it is convenient to represent in a unit system.

For each dimension, we choose a base unit. Our system's base units are grams, centimeters, seconds, Kelvin, and radian. All units can be described as combinations of these base dimensions along with a conversion factor to equivalent base units.

The choice of CGS as the base unit system is somewhat arbitrary. Most unit systems choose SI as the reference unit system. We use CGS to stay consistent with the rest of the `yt` codebase and to reflect the standard practice in astrophysics. In any case, using a **physical** coordinate system makes it possible to compare quantities and arrays produced by different datasets, possibly with different conversion factors to CGS and to code units. We go into more detail on this point below. In the future, we plan to make the preferred internal coordinate system a user-configurable option.

We provide `sympy Symbol` objects for the base dimensions. The dimensionality of all other units should be `sympy Expr` objects made up of the base dimension objects and the `sympy` operation objects `Mul` and `Pow`.

Let's use some common units as examples: `gram (g)`, `erg (erg)`, and solar mass per cubic megaparsec (`Msun / Mpc3`). `g` is an atomic, CGS base unit, `erg` is an atomic unit in CGS, but is not a base unit, and `Msun/Mpc3` is a combination of atomic units, which are not in CGS, and one of them even has an SI prefix. The dimensions of `g` are `mass` and the cgs factor is 1. The dimensions of `erg` are `mass * length2 * time-2` and the cgs factor is 1. The dimensions of `Msun/Mpc3` are `mass / length3` and the cgs factor is about 6.8e-41.

We use the `UnitRegistry` class to define all valid atomic units. All unit registries contain a unit symbol lookup table (dict) containing the valid units' dimensionality and cgs conversion factor. Here is what it would look like with the above units:

```
{ "g":      (mass, 1.0),
  "erg":    (mass * length**2 * time**-2, 1.0),
  "Msun":   (mass, 1.98892e+33),
  "pc":     (length, 3.08568e18), }
```

Note that we only define **atomic** units here. There should be no operations in the registry symbol strings. When we parse non-atomic units like `Msun/Mpc**3`, we use the registry to look up the symbols. The unit system in yt knows how to handle units like `Mpc` by looking up unit symbols with and without prefixes and modify the conversion factor appropriately.

We construct a `Unit` object by providing a string containing atomic unit symbols, combined with operations in Python syntax, and the registry those atomic unit symbols are defined in. We use sympy's string parsing features to create the unit expression from the user-provided string.

`Unit` objects are associated with four instance members, a unit `Expression` object, a dimensionality `Expression` object, a `UnitRegistry` instance, and a scalar conversion factor to CGS units. These data are available for a `Unit` object by accessing the `expr`, `dimensions`, `registry`, and `cgs_value` attributes, respectively.

`Unit` provides the methods `same_dimensions_as`, which returns `True` if passed a `Unit` object that has equivalent dimensions, `get_cgs_equivalent`, which returns the equivalent cgs base units of the `Unit`, and the `is_code_unit` property, which is `True` if the unit is composed purely of code units and `False` otherwise. `Unit` also defines the `mul`, `div`, `pow`, and `eq` operations with other unit objects, making it easy to compose compound units algebraically.

The `UnitRegistry` class provides the `add`, `remove`, and `modify` methods which allows users to add, remove, and modify atomic unit definitions present in `UnitRegistry` objects. A dictionary lookup table is also attached to the `UnitRegistry` object, providing an interface to look up unit symbols. In general, unit registries should only be adjusted inside of a code frontend, since otherwise quantities and arrays might be created with inconsistent unit metadata. Once a unit object is created, it will not receive updates if the original unit registry is modified.

## Creating YTArray and YTQuantity instances

There are two ways to create new array and quantity objects: via a constructor, and by multiplying scalar data by a unit quantity.

### Class Constructor

The primary internal interface for creating new arrays and quantities is through the class constructor for `YTArray`. The constructor takes three arguments. The first argument is the input scalar data, which can be an integer, float, list, or array. The second argument, `input_units`, is a unit specification which must be a string or `Unit` instance. Last, users may optionally supply a `UnitRegistry` instance, which will be attached to the array. If no `UnitRegistry` is supplied, a default unit registry is used instead. Unit specification strings must be algebraic combinations of unit symbol names, using standard Python mathematical syntax (i.e. `**` for the power function, not `^`).

Here is a simple example of `YTArray` creation:

```
>>> from yt.units import yt_array, YTQuantity
>>> YTArray([1, 2, 3], `cm`)
YTArray([1, 2, 3]) cm
>>> YTQuantity(3, `J`)
3 J
```

In addition to the class constructor, we have also defined two convenience functions, `quan`, and `arr`, for quantity and array creation that are attached to the `Dataset` base class. These were added to syntactically simplify the creation of arrays with the `UnitRegistry` instance associated with a dataset. These functions work exactly like the `YTArray` and `YTQuantity` constructors, but pass the `UnitRegistry` instance attached to the dataset to the underlying constructor call. For example:

```
>>> import yt
>>> ds = yt.load(`Enzo_64/DD0043/data0043`)
>>> ds.arr([1, 2, 3], `code_length`).in_cgs()
YTArray([ 5.55e+26, 1.11e+27, 1.66e+27]) cm
```

This example illustrates that the array is being created using `ds.unit_registry`, rather than the `default_unit_registry`, for which `code_length` is equivalent to `cm`.

## Multiplication

New `YTArray` and `YTQuantity` instances can also be created by multiplying `YTArray` or `YTQuantity` instances by `float` or `ndarray` instances. To make it easier to create arrays using this mechanism, we have populated the `yt.units` namespace with predefined `YTQuantity` instances that correspond to common unit symbol names. For example:

```

>>> from yt.units import meter, gram, kilogram, second, joule
>>> kilogram * meter**2 == joule
True
>>> from yt.units import m, kg, s, W
>>> kg*m**2/s**3 == W
True

>>> from yt.units import kilometer
>>> three_kilometers = 3*kilometer
>>> print three_kilometers
3.0 km

>>> from yt.units import gram, kilogram
>>> print gram+kilogram
1001.0 g
>>> print kilogram+gram
1.001 kg
>>> print kilogram/gram
1000.0 dimensionless

```

## Handling code units

Code units are tightly coupled to on-disk parameters. To handle this fact of life, the `yt` unit system can modify, add, and remove unit symbols via the `UnitRegistry`.

## Associating arrays with a coordinate system

To create quantities and arrays in units defined by a simulation coordinate system, we associate a `UnitRegistry` instance with `Dataset` instances. This unit registry contains the metadata necessary to convert the array to CGS from some other known unit system and is available via the `unit_registry` attribute that is attached to all `Dataset` instances.

We have modified the definition for `set_code_units` in the `StaticOutput` base class. In this new implementation, the predefined `code_mass`, `code_length`, `code_time`, and `code_velocity` symbols are adjusted to the appropriate values and `length_unit`, `time_unit`, `mass_unit`, `velocity_unit` attributes are attached to the `StaticOutput` instance. If there are frontend specific code units they should also be defined in subclasses by extending this function.

## Mixing modified unit registries

It becomes necessary to consider mixing unit registries whenever data needs to be compared between disparate datasets. The most straightforward example where this comes up is a cosmological simulation time series, where the code units evolve with time. The problem is quite general — we want to be able to compare any two datasets, even if they are unrelated.

We have designed the unit system to refer to a physical coordinate system based on CGS conversion factors. This means that operations on quantities with different unit registries will always agree since the final calculation is always performed in CGS.

The examples below illustrate the consistency of this choice:

```
>>> import yt
>>> ds1 = yt.load('Enzo_64/DD0002/data0002')
>>> ds2 = yt.load('Enzo_64/DD0043/data0043')
>>> print ds1.length_unit, ds2.length_unit
128 Mpccm/h, 128 Mpccm/h
>>> print ds1.length_unit.in_cgs()
6.26145538088e+25 cm
>>> print ds2.length_unit.in_cgs()
5.55517285026e+26 cm

>>> print ds1.length_unit*ds2.length_unit
145359.100149 Mpccm**2
>>> print ds2.length_unit*ds1.length_unit
1846.7055432 Mpccm**2
```

For the last two examples, the answer is not the seemingly trivial  $128^2 = 16384, \text{Mpccm}^2/h^2$ . This is because the new quantity returned by the multiplication operation inherits the unit registry from the left object in binary operations. This convention is enforced for all binary operations on two `YTarray` objects. Results are always consistent when referencing an unambiguous physical coordinate system:

```
>>> print (pf1.length_unit * pf2.length_unit).in_cgs()
3.4783466935e+52 cm**2
>>> print pf1.length_unit.in_cgs() * pf2.length_unit.in_cgs()
3.4783466935e+52 cm**2
```

## Handling cosmological units

If we detect that we are loading a cosmological simulation performed in comoving coordinates, extra comoving units are added to the dataset's unit registry. Comoving length unit symbols are still named following the pattern `<length symbol>cm`, i.e. `Mpccm`.

The  $h$  symbol is treated as a base unit, `h`, which defaults to unity. The `Dataset.set_units` updates the `h` symbol to the correct value when loading a cosmological simulation.

## User-Friendliness

---

### Publication-Ready Figures

### Jupyter Integration

### Halo-Finding and Catalogs

---

### Scaling and Parallelism

---

## Performance of Operations

### Inline Analysis

### Simple Parallelism

## Analysis Modules

---

## Extensions and Ecosystem

---

### Trident

Trident [\[31\]](#) is a Python-based open-source tool for post-processing hydrodynamical simulations to produce synthetic absorption spectra and related data. In many ways, Trident is the first external package that utilizes `yt` to provide data access and numerical operations, but then builds on those to develop detailed, astrophysically-aware systems for processing and analyzing that data.

### Powderday

[\[32\]](#)

### ytree

Building on `yt` for access to halo catalogs, and implementing a similar system for derived fields as applied to graph datasets, ytree [\[33\]](#) is a system for analyzing merger trees from analysis of dark matter halos in cosmological simulations.

ytree provides flexibility in determining the path that a given analysis takes through the graph of merger trees; for instance, it enables the user to select if they wish to follow the “most massive” progenitor halo backwards in time, or even to set their own criteria for this. Connecting this to the raw, unprocessed data from the simulation (such as the unsampled particle or cell content that comprises the halos) allows researchers to deepen and guide their analysis based on the physical characteristics of the merger history.

## Future Directions

---



## References

---

**1. Python utilities for Manubot: Manuscripts, open and automated: manubot/manubot**

Manubot

(2019-07-11) <https://github.com/manubot/manubot>

**2. yt: A MULTI-CODE ANALYSIS TOOLKIT FOR ASTROPHYSICAL SIMULATION DATA**

Matthew J. Turk, Britton D. Smith, Jeffrey S. Oishi, Stephen Skory, Samuel W. Skillman, Tom Abel, Michael L. Norman

*The Astrophysical Journal Supplement Series* (2010-12-28) <https://doi.org/ft6md2>

DOI: [10.1088/0067-0049/192/1/9](https://doi.org/10.1088/0067-0049/192/1/9)

**3. Petascale Cosmology: Simulations of Structure Formation**

Rupert Croft, Tiziana Di Matteo, Nishikanta Khandai

*Comput. Sci. Eng.* (2015-03) <http://ieeexplore.ieee.org/lpdocs/epic03/wrapper.htm?arnumber=7006381>

DOI: [10.1109/mcse.2015.5](https://doi.org/10.1109/mcse.2015.5)

**4. The LSST Data Management System**

Mario Jurić, Jeffrey Kantor, K-T Lim, Robert H. Lupton, Gregory Dubois-Felsmann, Tim Jenness, Tim S. Axelrod, Jovan Aleksić, Roberta A. Allsman, Yusra AlSayyad, ... LSST Project

*eprint arXiv:1512.07914* (2015) <http://adsabs.harvard.edu/abs/2015arXiv151207914J>

**5. A computer oriented geodetic data base and a new technique in file sequencing**

G. M. Morton

*IBM Ltd.* (1996)

**6. Gesammelte Abhandlungen: Band III: Analysis - Grundlagen der Mathematik Physik - Verschiedenes Lebensgeschichte**

David Hilbert

*Springer Berlin Heidelberg* (1970) [http://dx.doi.org/10.1007/978-3-662-25726-5\\_{\\\_}1](http://dx.doi.org/10.1007/978-3-662-25726-5_{\_}1)

DOI: [10.1007/978-3-662-25726-5\\_1](https://doi.org/10.1007/978-3-662-25726-5_1) · ISBN: [978-3-662-25726-5](https://doi.org/978-3-662-25726-5)

**7. The cosmological simulation code gadget-2**

Volker Springel

*Mon. Not. R. Astron. Soc.* (2005-12) <http://adsabs.harvard.edu/abs/2005MNRAS.364.1105S>

DOI: [10.1111/j.1365-2966.2005.09655.x](https://doi.org/10.1111/j.1365-2966.2005.09655.x)

**8. Cosmological Hydrodynamics with Adaptive Mesh Refinement: a new high resolution code called RAMSES**

Romain Teyssier

*Astron. Astrophys.* v.385, p.337-364 (2001-11) <http://arxiv.org/abs/astro-ph/0111367>

<http://dx.doi.org/10.1051/0004-6361:20011817>

DOI: [10.1051/0004-6361:20011817](https://doi.org/10.1051/0004-6361:20011817)

**9. Speeding up construction of PMR quadtree-based spatial indexes**

Gisli R. Hjaltason, Hanan Samet

*VLDB J. Int. J. Very Large Data Bases* (2002-10) <http://link.springer.com/10.1007/s00778-002-0067-8>

DOI: [10.1007/s00778-002-0067-8](https://doi.org/10.1007/s00778-002-0067-8)

**10. Fast construction of k-nearest neighbor graphs for point clouds.**

Michael Connor, Piyush Kumar

*IEEE Trans. Vis. Comput. Graph.* (2010-01) <http://www.ncbi.nlm.nih.gov/pubmed/20467058>  
DOI: [10.1109/tvcg.2010.9](https://doi.org/10.1109/tvcg.2010.9) · PMID: [20467058](https://pubmed.ncbi.nlm.nih.gov/20467058/)

### 11. A class of data structures for associative searching

J. A. Orenstein, T. H. Merrett

*Proc. 3rd acm sigact-sigmod symp. Princ. Database syst. - pod. '84* (1984-04)

<http://dl.acm.org/citation.cfm?id=588011.588037>

DOI: [10.1145/588011.588037](https://doi.org/10.1145/588011.588037) · ISBN: [0897911288](https://www.isbn-international.org/product/0897911288)

### 12. Encoded bitmap indexing for data warehouses

Ming-Chuan Wu, A. P. Buchmann

*Proc. 14th int. Conf. Data eng.* (1998) <http://ieeexplore.ieee.org/lpdocs/epic03/wrapper.htm?arnumber=655780>

DOI: [10.1109/icde.1998.655780](https://doi.org/10.1109/icde.1998.655780) · ISBN: [0-8186-8289-2](https://www.isbn-international.org/product/0818682892)

### 13. Bitmap index design and evaluation

Chee-Yong Chan, Yannis E. Ioannidis

*ACM SIGMOD Rec.* (1998-06) <http://dl.acm.org/citation.cfm?id=276305.276336>

DOI: [10.1145/276305.276336](https://doi.org/10.1145/276305.276336) · ISBN: [0-89791-995-5](https://www.isbn-international.org/product/0897919955)

### 14. An efficient bitmap encoding scheme for selection queries

Chee-Yong Chan, Yannis E. Ioannidis

*ACM SIGMOD Rec.* (1999-06) <http://dl.acm.org/citation.cfm?id=304181.304201>

DOI: [10.1145/304181.304201](https://doi.org/10.1145/304181.304201) · ISBN: [1-58113-084-8](https://www.isbn-international.org/product/1581130848)

### 15. Evaluating Geospatial Geometry and Proximity Queries Using Distributed Hash Tables

Matthew Malensek, Sangmi Pallickara, Shrideep Pallickara

*Comput. Sci. Eng.* (2014-07) <http://ieeexplore.ieee.org/lpdocs/epic03/wrapper.htm?arnumber=6785924>

DOI: [10.1109/mcse.2014.48](https://doi.org/10.1109/mcse.2014.48)

### 16. Bitmap indexes for large scientific data sets: a case study

R. R. Sinha, S. Mitra, M. Winslett

*Proc. 20th ieee int. Parallel distrib. Process. Symp.* (2006)

<http://ieeexplore.ieee.org/lpdocs/epic03/wrapper.htm?arnumber=1639304>

DOI: [10.1109/ipdps.2006.1639304](https://doi.org/10.1109/ipdps.2006.1639304) · ISBN: [1-4244-0054-6](https://www.isbn-international.org/product/1424400546)

### 17. Multi-resolution bitmap indexes for scientific data

Rishi Rakesh Sinha, Marianne Winslett

*ACM Trans. Database Syst.* (2007-08) <http://portal.acm.org/citation.cfm?doid=1272743.1272746>

DOI: [10.1145/1272743.1272746](https://doi.org/10.1145/1272743.1272746)

### 18. Improving the Performance of High-Energy Physics Analysis through Bitmap Indices

Kurt Stockinger, Dirk Duellmann, Wolfgang Hoschek, Erich Schikuta

*Database expert syst. Appl. 11th int. Conf. DEXA 2000 london, uk, sept. 4-8, 2000 proc.* (2000-06)  
<http://link.springer.com/10.1007/3-540-44469-6>

DOI: [10.1007/3-540-44469-6](https://doi.org/10.1007/3-540-44469-6) · ISBN: [978-3-540-67978-3](https://www.isbn-international.org/product/9783540679783)

### 19. Using bitmap index for interactive exploration of large datasets

Kesheng Wu, W. Koegler, J. Chen, A. Shoshani

*15th int. Conf. Sci. Stat. Database manag. 2003.* (2003) <http://ieeexplore.ieee.org/articleDetails.jsp?arnumber=1214955>

DOI: [10.1109/ssdm.2003.1214955](https://doi.org/10.1109/ssdm.2003.1214955) · ISBN: [0-7695-1964-4](https://www.isbn-international.org/product/0769519644)

## 20. Range-based bitmap indexing for high cardinality attributes with skew

P. S. Yu

*Proceedings. Twenty-second annu. Int. Comput. Softw. Appl. Conf. (Compsac '98) (cat. No.98CB 36241)* (1998) <http://ieeexplore.ieee.org/lpdocs/epic03/wrapper.htm?arnumber=716637>

DOI: [10.1109/compsac.1998.716637](https://doi.org/10.1109/compsac.1998.716637) · ISBN: [0-8186-8585-9](https://www.isbn-international.org/product/0-8186-8585-9)

## 21. Multidimensional indexing and query coordination for tertiary storage management

A. Shoshani, L. M. Bernardo, H. Nordberg, D. Rotem, A. Sim

*Proceedings. Elev. Int. Conf. Sci. Stat. Database manag.* (1999)

<http://ieeexplore.ieee.org/lpdocs/epic03/wrapper.htm?arnumber=787637>

DOI: [10.1109/ssdm.1999.787637](https://doi.org/10.1109/ssdm.1999.787637) · ISBN: [0-7695-0046-3](https://www.isbn-international.org/product/0-7695-0046-3)

## 22. Evaluation Strategies for Bitmap Indices with Binning

Kurt Stockinger, Kesheng Wu, Arie Shoshani

*Database expert syst. Appl. 15th int. Conf. DEXA 2004, zaragoza, spain, august 30-september 3, 2004.*

*Proc.* (2004) [http://dx.doi.org/10.1007/978-3-540-30075-5\\_12](http://dx.doi.org/10.1007/978-3-540-30075-5_12)

DOI: [10.1007/978-3-540-30075-5\\_12](https://doi.org/10.1007/978-3-540-30075-5_12) · ISBN: [978-3-540-30075-5](https://www.isbn-international.org/product/978-3-540-30075-5)

## 23. Compressed bitmap indices for efficient query processing

Kesheng Wu, Ekow Otoo, Arie Shoshani

*Lawrence Berkeley Natl. Lab.* (2001-09) <http://escholarship.org/uc/item/8k22w7q2>

## 24. Sorting improves word-aligned bitmap indexes

Daniel Lemire, Owen Kaser, Kamel Aouiche

*Data Knowl. Eng.* (2010-01) <http://dl.acm.org/citation.cfm?id=1663645.1663682>

DOI: [10.1016/j.datak.2009.08.006](https://doi.org/10.1016/j.datak.2009.08.006)

## 25. Compressed bitmap indexes: beyond unions and intersections

Owen Kaser, Daniel Lemire

*Softw. Pract. Exp.* (2016-02) <http://doi.wiley.com/10.1002/spe.2289>

DOI: [10.1002/spe.2289](https://doi.org/10.1002/spe.2289)

## 26. Smoothed Particle Hydrodynamics

J. J. Monaghan

*Annu. Rev. Astron. Astrophys.* (1992-09) <http://adsabs.harvard.edu/abs/1992ARA...A..30..543M>

DOI: [10.1146/annurev.aa.30.090192.002551](https://doi.org/10.1146/annurev.aa.30.090192.002551)

## 27. GADGET: a code for collisionless and gasdynamical cosmological simulations

Volker Springel, Naoki Yoshida, Simon D. M. White

*New Astron.* (2001-04) <http://adsabs.harvard.edu/abs/2001NewA....6...79S>

DOI: [10.1016/s1384-1076\(01\)00042-2](https://doi.org/10.1016/s1384-1076(01)00042-2)

## 28. A new class of accurate, mesh-free hydrodynamic simulation methods

P. F. Hopkins

*Mon. Not. R. Astron. Soc.* (2015-04) <http://adsabs.harvard.edu/abs/2014arXiv1409.7395H>

DOI: [10.1093/mnras/stv195](https://doi.org/10.1093/mnras/stv195)

## 29. yt: A MULTI-CODE ANALYSIS TOOLKIT FOR ASTROPHYSICAL SIMULATION DATA

Matthew J. Turk, Britton D. Smith, Jeffrey S. Oishi, Stephen Skory, Samuel W. Skillman, Tom Abel, Michael L. Norman

*Astrophys. J. Suppl. Ser.* (2011-01) [http://stacks.iop.org/0067-0049/192/i=1/a=9?](http://stacks.iop.org/0067-0049/192/i=1/a=9?key=crossref.ad58f4fc8c6272d93975507bf0238006)

[key=crossref.ad58f4fc8c6272d93975507bf0238006](http://stacks.iop.org/0067-0049/192/i=1/a=9?key=crossref.ad58f4fc8c6272d93975507bf0238006)

DOI: [10.1088/0067-0049/192/1/9](https://doi.org/10.1088/0067-0049/192/1/9)

### 30. **Cython: The Best of Both Worlds**

Stefan Behnel, Robert Bradshaw, Craig Citro, Lisandro Dalcin, Dag Sverre Seljebotn, Kurt Smith  
*Comput. Sci. Eng.* (2011-03) <http://ieeexplore.ieee.org/lpdocs/epic03/wrapper.htm?arnumber=5582062>  
DOI: [10.1109/mcse.2010.118](https://doi.org/10.1109/mcse.2010.118)

### 31. **Trident: A Universal Tool for Generating Synthetic Absorption Spectra from Astrophysical Simulations**

Cameron B. Hummels, Britton D. Smith, Devin W. Silvia  
*The Astrophysical Journal* (2017-09-20) <https://doi.org/gcx4th>  
DOI: [10.3847/1538-4357/aa7e2d](https://doi.org/10.3847/1538-4357/aa7e2d)

### 32. **The formation of submillimetre-bright galaxies from gas infall over a billion years**

Desika Narayanan, Matthew Turk, Robert Feldmann, Thomas Robitaille, Philip Hopkins, Robert Thompson, Christopher Hayward, David Ball, Claude-André Faucher-Giguère, Dušan Kereš  
*Nature* (2015-09) <https://doi.org/f7r445>  
DOI: [10.1038/nature15383](https://doi.org/10.1038/nature15383) · PMID: [26399829](https://pubmed.ncbi.nlm.nih.gov/26399829/)

### 33. **Ytree: Merger-Tree Toolkit**

Britton Smith, Meagan Lang  
*Zenodo* (2018-02-16) <https://doi.org/gcx4x2>  
DOI: [10.5281/zenodo.1174374](https://doi.org/10.5281/zenodo.1174374)

## Conclusions

---

## Acknowledgments

---

The authors of this paper would like to extend their deepest gratitude to the many, many individual and institutions that have contributed, directly or indirectly, to the growth of both `yt` and the `yt` community.

We particularly thank KIPAC and SLAC at Stanford, the University of California at San Diego and Santa Cruz, the High-Performance Astro Computing Center, Columbia University, the University of Illinois, University of Colorado at Boulder, University of Edinburgh, the scientific python community, NumFOCUS,